



# Underperforming light curing procedures trigger detrimental irradiance-dependent biofilm response on incrementally placed dental composites

Haifa Maktabi<sup>a</sup>, Maria Ibrahim<sup>b</sup>, Qoot Alkhubaizi<sup>a</sup>, Michael Weir<sup>b</sup>, Hockin Xu<sup>b</sup>, Howard Strassler<sup>a</sup>, Ana Paula P. Fugolin<sup>c</sup>, Carmem S. Pfeifer<sup>c</sup>, Mary Anne S. Melo<sup>a,b,\*</sup>

<sup>a</sup> Division of Operative Dentistry, Department of General Dentistry, University of Maryland School of Dentistry, Baltimore, MD 21201, USA

<sup>b</sup> Ph.D. Program in Biomedical Sciences, Division of Biomaterials & Tissue Engineering, Dept. of Advanced Oral Sciences and Therapeutics, University of Maryland Dental School, Baltimore, MD 21201, USA

<sup>c</sup> Division of Biomaterials and Biomechanics, Department of Restorative Dentistry, School of Dentistry, Oregon Health & Science University, Portland, OR 97239, USA

## ARTICLE INFO

### Keywords:

Light curing  
The degree of conversion  
*S. mutans*  
Oral biofilm  
Resin composite

## ABSTRACT

**Objectives:** Insufficient radiant exposure ( $J/cm^2$ ) may provide an early trigger in a cascade of detrimental responses on incrementally-place composite, especially the bottom layer. This study aimed to assess the influence of poor radiant exposure, the degree of conversion (%DC), water sorption/ solubility and *S. mutans* biofilm formation on conventional, incrementally placed composites and to establish a relationship between these factors.

**Methods:** Two light units operating at 600 and 1000  $mW/cm^2$  and four most common operator-dependent curing conditions had the radiant exposure ( $R_E$ ) recorded. All the specimens were subjected to *S. mutans* biofilm model for 14 days. The %DC, biofilm formation expressed by colony-forming units (CFU), water sorption/ solubility and surface roughness/ SEM were assessed. Data were submitted to two-way ANOVA and Tukey post-hoc test ( $\alpha = 0.05$ ). Pearson correlation was also determined.

**Results:** The influence of  $R_E$  on *S. mutans* CFU values and DC are dependent on the curing conditions and irradiance ( $p < 0.05$ ). A negative relationship was observed between  $R_E$  and biofilm formation. The operator-dependent curing conditions have shown  $R_E$  reduction varying from 49.4% to 73.5% in relation to control. The difference in DC between top/bottom of cylinder varied from 13% to 21% for 1000  $mW/cm^2$  and from 29% to 53% for LCU600. The roughness, solubility and salivary sorption were greater for low  $R_E$ .

**Conclusion:** Poor, deficient curing procedures provide an early trigger in a negative pathway of events for incrementally-place dental composite including a biological response by increased biofilm formation by *S. mutans*, a relevant factor for secondary caries development.

**Significance:** The susceptibility to variation in the outcomes was  $R_E$ -dependent. The optimization of the curing procedures ensures the maximum performance in the chain of events involved in the light curing process of resin-based materials and potentially reduce the risk factors of secondary caries development.

## 1. Introduction

One long-time drawback of dental composites is that they are more prone to biofilm accumulation and plaque formation than amalgam and glass ionomer restorative materials [1]. The ester-containing methacrylate in their chemical composition makes restorative dental polymers prone to degradation by bacterial acids and enzymatic hydrolytic activity present in the oral cavity. Some products of composite biodegradation have also been shown to promote the growth of *Streptococcus mutans*, a dominant cariogenic bacterium. [2,3]. The bacterial colonization of the composite restoration may lead to failure of restoration

-tooth interface and, consequently, caries formation around the composite restorations [4]. Secondary caries is one of the main reasons for restoration failure reported in clinical trials [5,6].

Currently, resin composites are cured by light-induced polymerization of methacrylate monomers [7]. Those materials form highly crosslinked networks and reach gelation and vitrification at relatively low conversions, which causes the limiting conversions to be only around 50 to 70% [8,9], even for materials where the curing procedures are optimized. Cumulative evidence from studies of resin composite/ cariogenic bacteria interactions has suggested that residual unpolymerized monomers that leach from the composite may primarily

\* Corresponding author at: Operative Dentistry Division, Department of General Dentistry, University of Maryland School of Dentistry, Baltimore, MD 21201, USA.  
E-mail address: [Mmelo@umaryland.edu](mailto:Mmelo@umaryland.edu) (M.A.S. Melo).

stimulate *S. mutans* adherence, colonization, and growth over the composite. [10,11]. Recently, more insightful mechanistic pathway findings have highlighted the relationship of by-products released from adequately cured resin composites and their influence in the *S. mutans* biofilm growth [12,13]. There is a rapidly expanding body of evidence suggesting the role of uncured monomers on the promotion of growth of cariogenic species and the possibility of the eluted monomers accelerating the growth of bacteria over restorative materials [13,14,16]. Another relevant factor to consider, it is the potential role of product-derived from degradation on *S. mutans* virulence-associated gene [16,17]. Although, the emergent research on interactions of dental monomers with biological systems in the oral cavity indicates changes in *S. mutans* biofilms in response to the dental composite degradation with ideal and standardized polymerization conditions, the potential detrimental effect of inadequate polymerization with increased release of uncured monomers could even demonstrate greater impact for the cariogenic biofilm-related implications. While investigations of such mechanistic in-depth factors are beyond the scope of this article, an examination of the influence of poor radiant exposure on *S. mutans* biofilm formation is presented.

Insufficient radiant exposure ( $J/cm^2$ ), due to poor curing procedures, may trigger a snowball effect driving to shorten the long-term lifetime service of composites [18]. Incomplete conversion of the polymer matrix, significant release of materials to the oral environment, high degradation upon oral fluids, increase of water sorption and increase roughness is the potential pathway of detrimental events leading to the increase of biofilm accumulation and, consequentially, the risk of development of caries lesions around restorations (CARS) due to inappropriate curing procedures of the material [19].

The radiant exposure ( $J/cm^2$ ) delivered to the composites during the curing procedures contributes to the properties of the resin based-materials [20]. Insufficient delivered radiant exposure may impart inadequate polymerization and indirectly has been suggested to adversely affect patients' long-term quality of dental composite restorations [21]. Certain conditions such as the distance of the light source, the direction of the light, the movement during the light curing procedure are operator-related factors that profoundly impacts the amount of radiant exposure received during the curing procedures [22]. Often it is straightforward to see a link between the radiant exposure and polymerization performance expressed by the degree of conversion of resin-based materials. Expressive literature has investigated the impact of irradiance on the degree of conversion of the monomers [20,24], but there are no studies examining the biofilm-related implications by means of correlation with inefficient polymerization resulting of poor performance of the curing procedures and variations in the irradiance.

This cited evidence motivated the present study to investigate the effect of the radiant exposure generated by less than optimal light curing conditions and different irradiances on the formation of *S. mutans* biofilm over composite surfaces. The degree of conversion, surface roughness and physical properties of a conventional composite were also assessed.

The tested null hypothesis was that the different levels of irradiance/light curing unit and radiant exposure promoted by underperformed curing conditions will not interfere with *S. mutans* biofilm formation (CFU), the degree of conversion (DC), the surface roughness (SR), water sorption and solubility.

## 2. Materials and methods

### 2.1. Experimental design

This *in vitro* study (Fig.1) has considered two light curing units operating at 600 and 1000 mW/cm<sup>2</sup> (LCU600 and LCU1000) and four curing conditions: (1) optimal- no light tip angulation and no separation between the tip and the surface of the specimen; (2) light tip angulation ( $\alpha = 20^\circ$ ); (3) light tip angulation ( $\alpha = 35^\circ$ ); (4) light tip 2 mm

away from the surface of the specimen. These conditions were determined in a previous study as the most common operator-dependent scenarios [22]. The irradiance conditions are illustrated in Fig. 1. The response variables were radiant exposure ( $R_E$  in  $J/cm^2$ ), the degree of conversion (%DC) on the top and bottom of specimens, colony-forming units (CFU/composite), the surface roughness ( $\mu m$ ) and water sorption/solubility ( $\mu g/mm^3$ ).

Two light curing units (LCU), representative of common irradiance available for dentists for curing composites were used. LCU600 provide the irradiance of LCU<sub>600</sub> (Radii-cal, SDI Limited Victoria, Australia; standard curing mode, irradiance output provided of 689 mW/cm<sup>2</sup>) and LCU1000 displayed 1000 mW/cm<sup>2</sup> (Valo grand, Ultradent Products Inc, South Jordan, UT, USA; standard curing mode; irradiance output provided of 1029 mW/cm<sup>2</sup>), respectively. A hybrid composite applied in a 2-mm increment was used in all tested conditions (Amelogen® Plus, Ultradent Products Inc). According to the manufacturer, the composite contains in percentage by weight, approximately 60 wt.% Bisphenol A-Glycidyl Methacrylate (Bis-GMA), 40 wt.% triethylene glycol dimethacrylate (TEGMA), 1 wt.% butylated hydroxytoluene (BHT) and 35 wt.% barium aluminosilicate glass powder as a filler.

### 2.2. Sample preparation and measurement of $R_E$ at the bottom surface of the specimen

To achieve uniformization during the simulation of variations in the way LCUs are handled during the curing of a posterior composite, templates were designed, and 3D printed creating less than optimal curing conditions as shown in Fig. 1. The 3D printed molds (polylactic acid filament, melted Extrusion Modeling, 3D H800 Afinia printer) were prepared with inner diameter = 7 mm and thickness = 2 mm. Initially, the radiant exposure ( $R_E$ ) values obtained with the curing unit placed either directly on the sensor, or the top of the empty mold was determined. Then, the  $R_E$  reaching the bottom of composite cylinders under the four curing conditions described above was measured. Each mold containing uncured composite was placed over the bottom sensor of a laboratory-grade NIST-referenced USB4000 Spectrometer (MARC: Managing Accurate Resin Curing; System, Bluelight Analytics Inc., Halifax, Canada) and photopolymerized for 20 s using one of the two LED curing units at irradiance output of approximately 600 or LCU2 1000. After curing, all the composite cylinders were dry stored at 37 °C for 24 h.

The total energy delivered to the specimen stated as radiant exposure ( $R_E$ ) was calculated according to the following equations:

Total energy ( $J/cm^2$ ) also referred as radiance exposure = incident irradiance ( $mW/cm^2$ ) x time (seconds) where, incident irradiance ( $mW/cm^2$ ): radiant power of LCU (mW) divided by total irradiated surface area ( $cm^2$ ).

$$\frac{J(\text{Joules})}{cm^2} = \frac{mW}{cm^2} \times t(\text{sec})$$

### 2.3. *S. mutans* biofilm model

The cured specimens (n = 6) were subjected to the biofilm model [25] with modifications. *S. mutans* (ATCC 700610, UA159; American Type Culture, Manassas, VA) was used as inoculum according to a protocol approved by the University of Maryland Baltimore. *S. mutans* was selected because of its acidogenic and aciduric properties, correlation with caries development and ability to better attach and survive on the composite surface than other species [10,12].

In brief, a 150  $\mu l$  of *S. mutans* inoculum in brain heart infusion (BHI, Sigma-Aldrich, St. Louis, Missouri, USA) -glycerol solution (stored at  $-80^\circ C$ ) was spread on Columbia blood agar (BBL, Becton Dickinson, Allschwil, Switzerland), incubated over 48 h. *S. mutans* colonies were resuspended in 5 ml of BHI broth and incubated overnight at 37 °C under the aerobic condition to the mid-log phase ( $OD_{600} = 0.9$ ). The

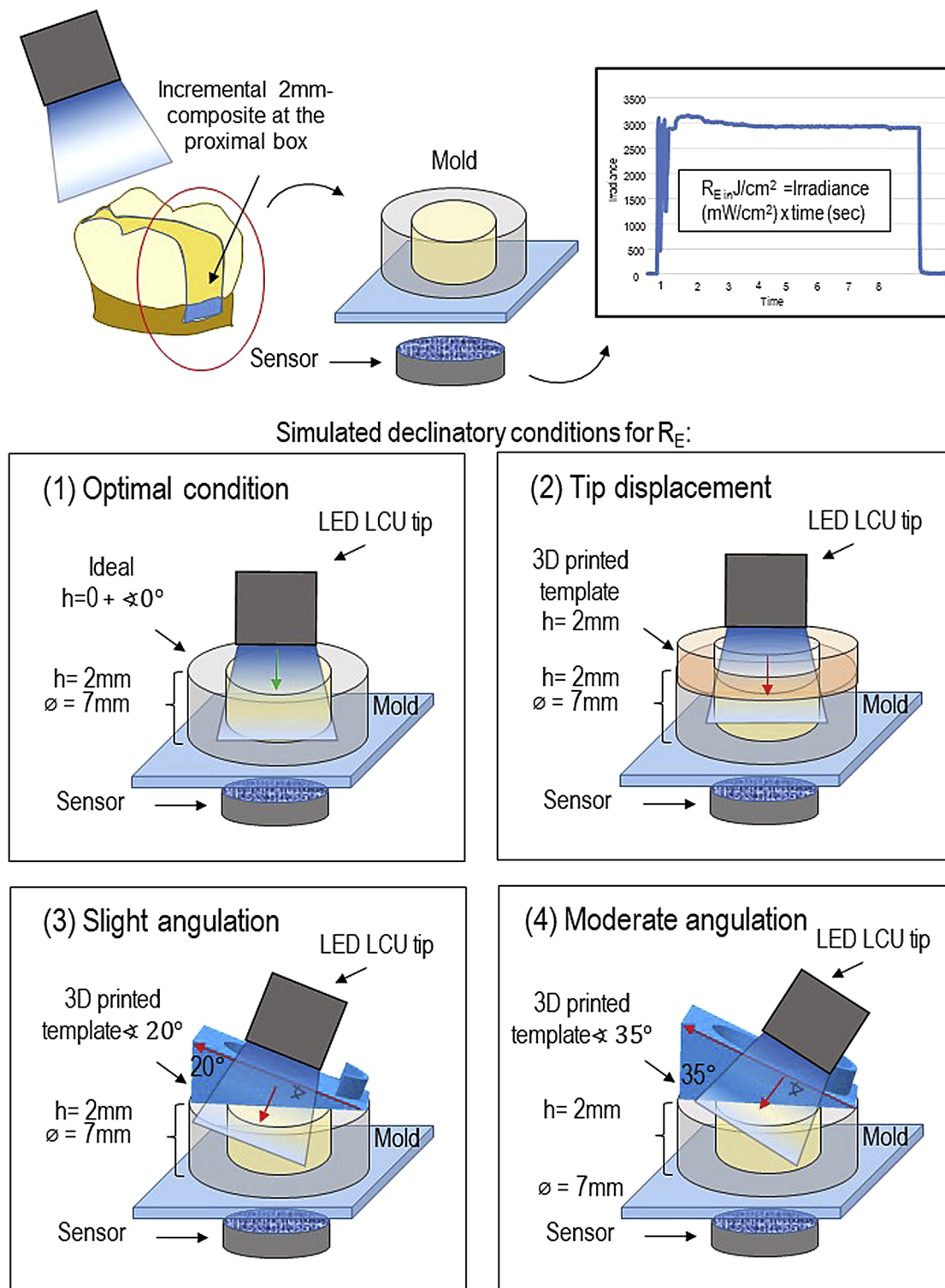


**Fig. 1.** Schematic representation of clinical simulated conditions in this experiment. Our 2-mm increment composite aims to represent the first increment of composite placed in the proximal box of a class II preparation. To light cure this increment, very often clinicians face downgrade conditions for light delivery such as tip displacement and angulation. Taking into consideration, samples were prepared and  $R_E$  at the bottom surface of the specimen was measured under the following simulated conditions: (1) optimal condition (no angulation or tip displacement), (2) tip-displacement (2 mm), (3) light tip angulation ( $\alpha = 20^\circ$ ) and (4) light tip angulation ( $\alpha = 35^\circ$ ).

composite cylinder ( $n = 6$ ) previously sterilized via ethylene oxide gas was placed in a well of a 24-well plate and immersed in sterile BHI containing 5% sucrose (w/v) [8]. All BHI-containing wells were inoculated with  $120\ \mu\text{l}$  of  $1\text{--}2 \times 10^8$  CFU/ml overnight cultures of *S. mutans*. Inoculation of each BHI-containing recipient was performed

only once on the first day, and the composite cylinders were transferred to a fresh medium every day for 14 days. Also, each BHI-containing recipient was streaked onto a new fresh BHI agar media plated and incubated at  $37^\circ\text{C}$  in an atmosphere of 10%  $\text{CO}_2$  for 24 h to check for purity. For microbiological analysis, biofilm formed on composite

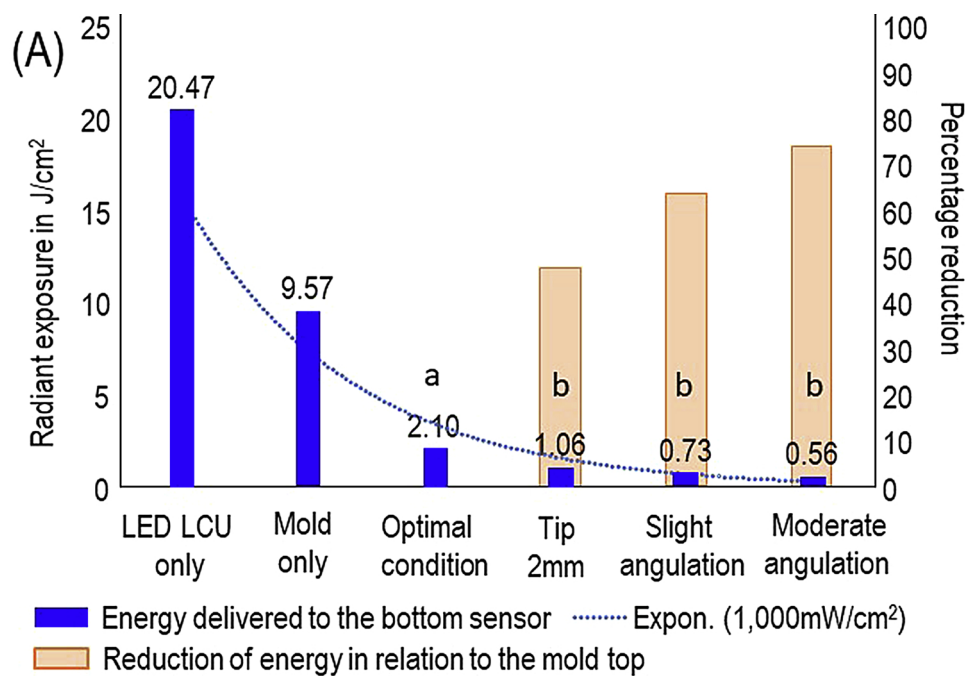
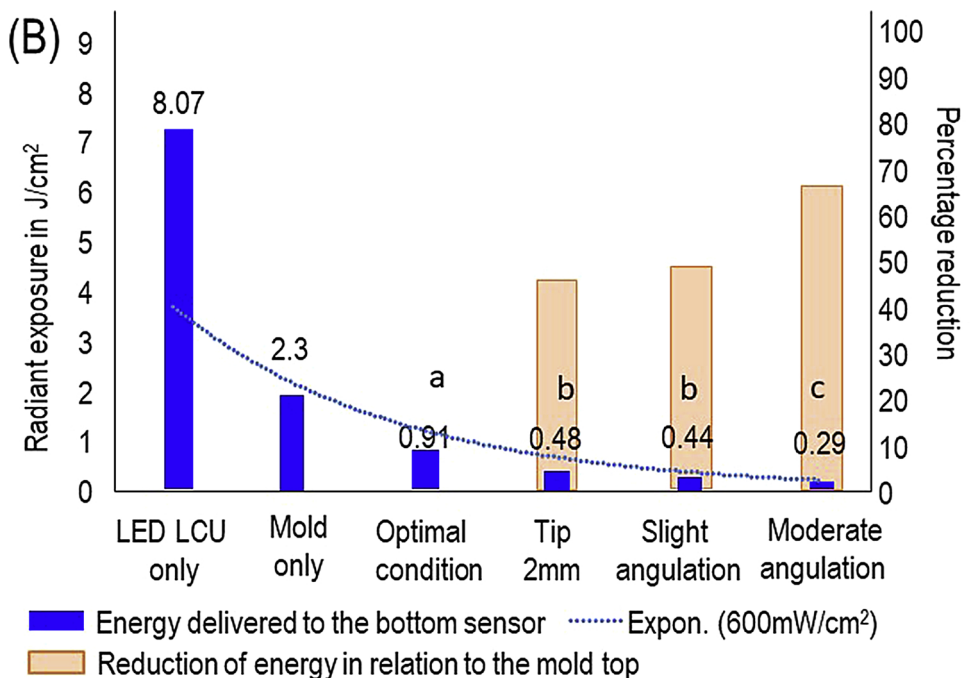


Fig. 2.  $R_E$  results and percentage reduction of  $R_E$  in relation to the  $R_E$  reached by applying the curing unit directly on the top of the mold without composite (mold only) considering the downgrade light conditions (mean  $\pm$  sd; n = 6) for: (A) LCU<sub>1000</sub> displaying irradiance output of 1000 mW/cm<sup>2</sup> and (B) LCU<sub>600</sub> representing irradiance output of 600 mW/cm<sup>2</sup>. The first y-axis, the barplot shows radiant exposure ( $R_E$ ) expressed in J/cm<sup>2</sup>. On the second y-axis, the barplot shows percentage reduction of  $R_E$ . The dotted line shows the exponential decay of RE for all groups in relation to radiant exposure ( $R_E$ ) reached by applying the curing unit directly on the sensor. In each plot, values with dissimilar letters are significantly different ( $p < 0.05$ ).



cylinders was collected, serially diluted with 0.9% sodium chloride (NaCl) solution and plated in triplicate on BHI agar. After 48 h at 37 °C in a 10% CO<sub>2</sub> atmosphere, representative colonies with typical morphology of *S. mutans* were counted using a colony counter and expressed as CFU/composite. To assess the single-examiner reliability, the data from the two attempts for microbiological assay using the two light units and the studied conditions were used. The first attempt was compared with a second attempt using paired *t*-test ( $\alpha = 0.05$ ), and no difference was found ( $p = 0.313$ ). Additionally, samples of control and moderate inclination condition were prepared for scanning electron microscopy (SEM, Quanta 200, FEI, Hillsboro, OR). Samples were sputter coated with gold/palladium and evaluated with a magnification of X200 and X10.000 at an accelerating voltage of 20 kV.

2.4. The degree of conversion analysis

The cylinders were stored in a dark container for 24 h at 37 °C A previous study has shown no significant effect of post-curing conversion after 24 h [26]. The cylinders were embedded into the epoxy resin (Die Epoxy Type 8000, American Dental Supply, INC, Allentown, PA) and sectioned using a diamond saw (Accutom-5, Struers, Cleveland, OH) to obtain three 0.4 mm thick slices parallel to the long axis of each cylinder (n = 3). The slices were positioned over the platform of an IR microscope (Nicolet Continuum) coupled with an IR spectrometer (Nicolet 6700, ThermoFisher, Madison, WI, USA). Spectra were obtained in near-IR at 0.5 mm steps through the 4 mm length of the specimen in transmission using the motorized stage of the microscope. Spectra of the uncured composite were used to calculate the vinyl

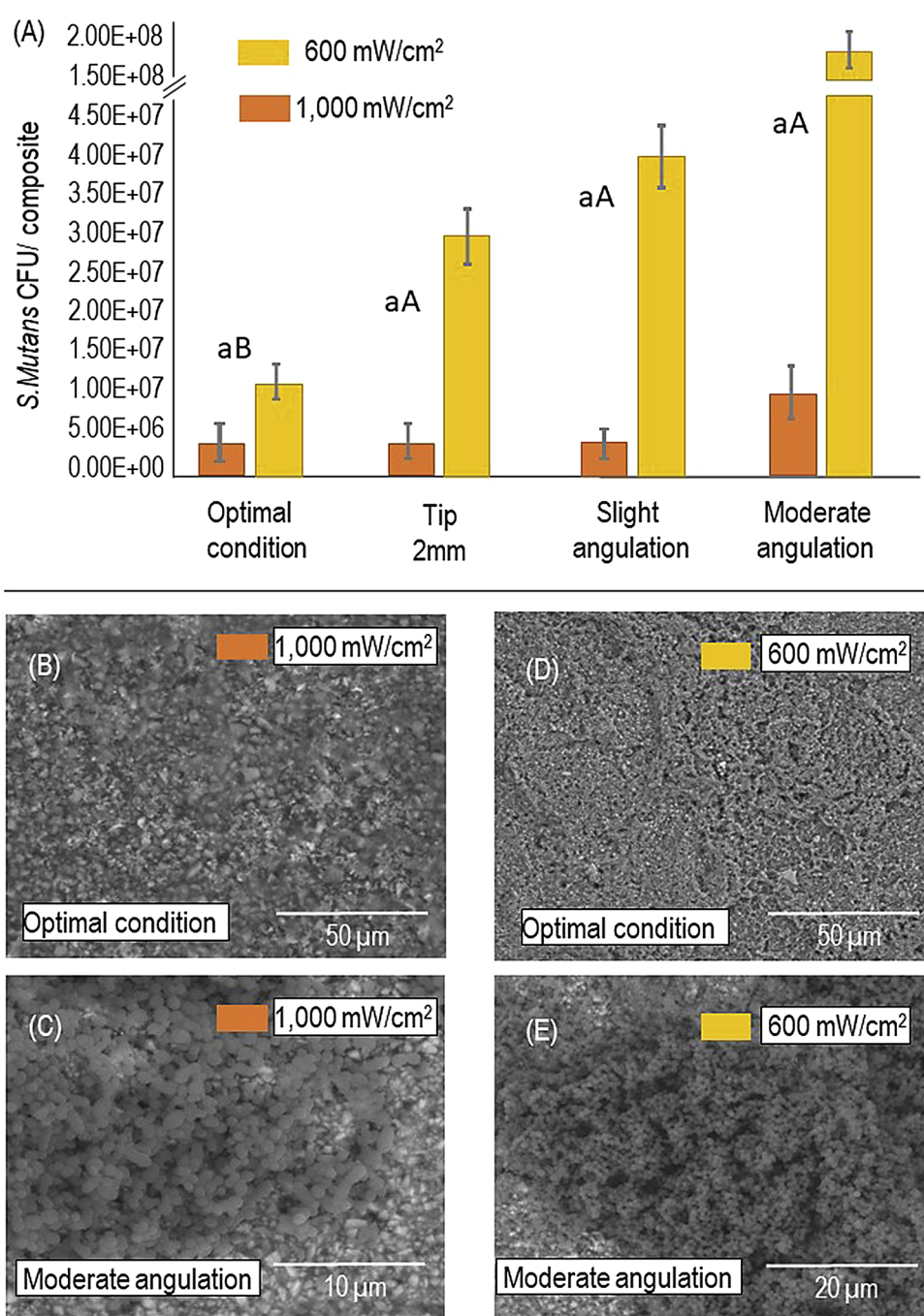


Fig. 3. (A) *S. mutans* counts CFU/ composite for each of irradiance output and downgrade light conditions (mean ± sd; n = 6); (B–C) Representative SEM images showing bacterial adhesion and biofilm formation on the bottom surfaces of composite cylinders for LCU1000 under control and moderate angulation, respectively and (D–E) representative SEM images showing increased *S. mutans* biofilm formation for LCU600 under control and moderate angulation. Capital letters compare LCU600, while lower case letters compare LCU2 1000.

double bond conversion at each depth using the vinyl overtone peak area at 6165 cm<sup>-1</sup> following previously published methods [27]. 2D maps of conversion as a function of depth were produced. The degree of conversion at each level was averaged and analyzed with two-way ANOVA, with a confidence level of 95%.

2.5. Surface roughness

Before and after the *S. mutans* biofilm model, the average surface roughness (Ra-μm) of the bottom of the composite cylinders (n = 6) were measured using a surface roughness measurement instrument (Surftest SJ-310; Mitutoyo America, Aurora, IL). The stylus tip (5 μm)

traversed the composite surface at a constant speed of 0.5 mm/s, the force of 4 mN, with a 0.25-mm cutoff value and 1.5-mm tracing length. The difference between the Ra final and Ra initial will be calculated and expressed as delta Ra (ΔRa). Additionally, samples of control and moderate inclination condition were prepared for SEM.

2.6. Water sorption and solubility

Composite samples (n = 6) were prepared and cured according to the tested curing conditions similar to the above-described method, and water sorption and solubility were assessed according to ISO 4049: 2009. Initially, the cured specimens were stored in desiccator drying

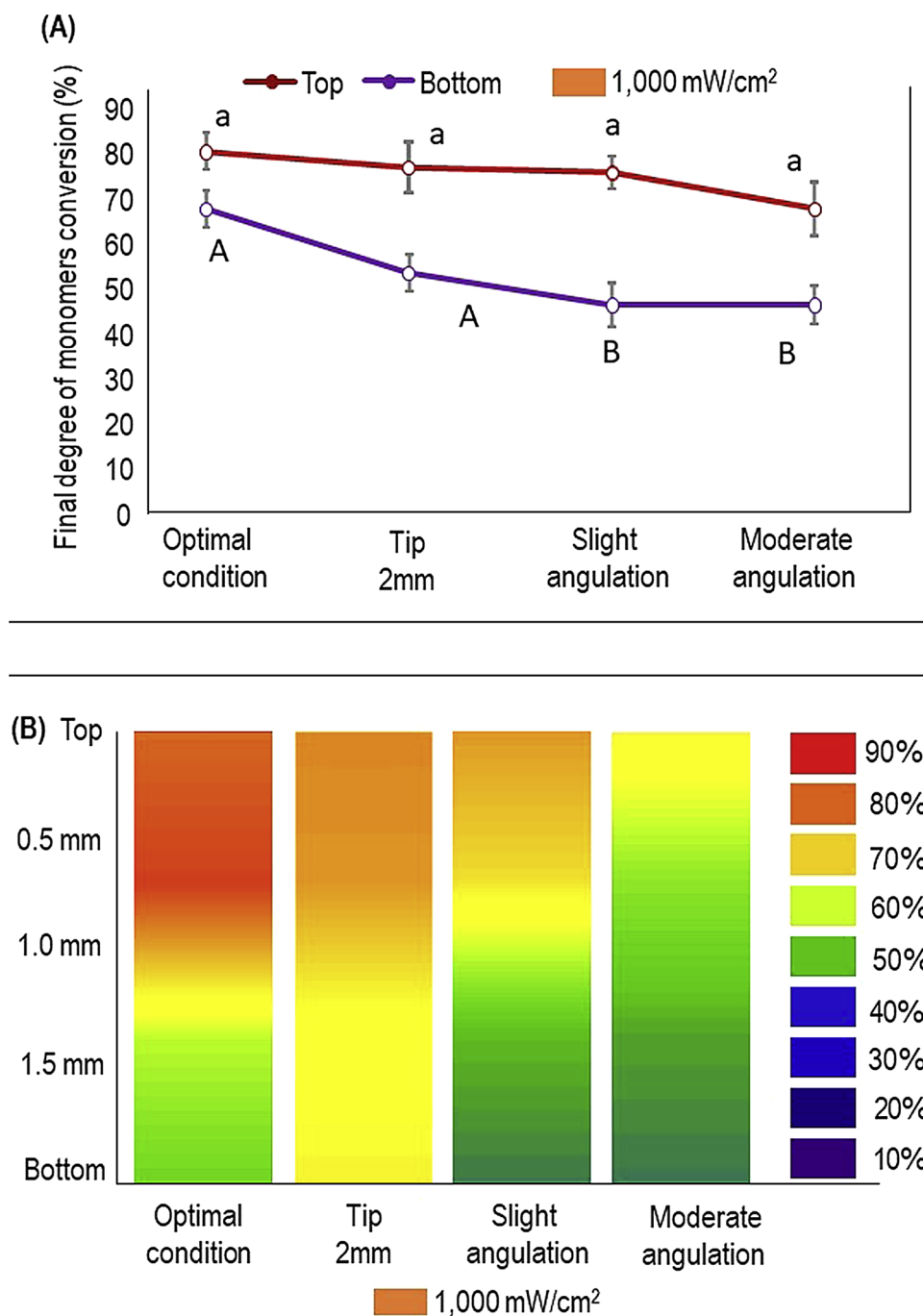


**Fig. 4.** The percentage and differences of the final DC for LCU2 1000 at the top and bottom in function of downgrade light conditions (mean ± sd; n = 3). In (A) the solid lines average the DC% values at the top and bottom. Lower case letters compare DC at the top, while capital case letters compare DC at the bottom. Dissimilar letters are significantly different ( $p < 0.05$ ). In (B), the heat maps of the average degree of conversion measured at different depths from irradiated surface to the bottom is illustrated. The color bar on the right shows the visual representation of % DC corresponding to the colors seen.

under vacuum over freshly dried silica gel at 37° for 22 h and then transferred to a desiccator at room temperature for 2 h before the initial weighting. Their masses were measured using an analytical balance with a precision of 0.001 g (U.S. Solid USS-DBS8). This cycle was repeated until a constant mass ( $m_1$ ) was obtained. Subsequently, cylinders were immersed in 10 ml of distilled water for seven days at 37 °C After the storage regime, composite cylinders were taken out, the excess water removed using a paper towel, and the specimen waved in the air at 23 °C for 15 s and reweighed ( $m_2$ ). Then, cylinders were dry-stored and the mass was daily recorded until a constant mass was obtained as described before ( $m_3$ ) [25]. The mean water sorption and

solubility of each specimen will be calculated according to Eqs. (1) and (2).

$$\text{Water sorption}(\%) = \frac{100(m^2 - m_1)}{m_1} \tag{1}$$

$$\text{Water solubility}(\%) = \frac{100(m_1 - m_3)}{m_1} \tag{2}$$

2.7. Statistical analysis

Statistical evaluations were performed with Stata 3.5 (Systat, San

Jose, CA). The Shapiro-Wilk test was applied to verify if the data were normally distributed. Results were compared using two-way ANOVA and Tukey HSD, ( $\alpha = 0.05$ ) where the factors under evaluation were light curing unit at 2 levels (LCU600 and LCU1000) and curing conditions at 4 levels (optimal, light tip angulation ( $\alpha = 20^\circ$ ); light tip angulation ( $\alpha = 35^\circ$ ) and light tip 2 mm away). The correlations between  $R_E$  and the outcomes properties were assessed by a linear Pearson correlation.

### 3. Results

Fig. 2 shows the  $R_E$  results and percentage reduction of  $R_E$  about the optimal condition (control) for each of irradiance output considering the less than optimal light conditions (mean  $\pm$  sd;  $n = 6$ ). In (A), the first y-axis, the barplot shows radiant exposure ( $R_E$ ) expressed in  $J/cm^2$  when LCU<sub>1000</sub> displaying irradiance output of  $1000\text{ mW/cm}^2$  was used. The influence of the less than optimal light conditions ( $r = 0.77$ ,  $p = 0.001$ ) and irradiance output of LCU ( $r = 0.85$ ,  $p = 0.001$ ) on the radiant exposure ( $R_E$ ) were significant.  $R_E$  values for the optimal condition were significantly different from all the other groups ( $p < 0.001$ ). On the second y-axis, the barplot shows the percentage reduction of  $R_E$ . The less than optimal light conditions have shown reduction varying from 49.4% to 73.5% in relation to optimal condition. The dotted line shows the exponential decay of  $R_E$  for all groups in relation to radiant exposure ( $R_E$ ) reached by applying the curing unit directly on the sensor. This decay illustrated the radiant emittance attenuation due to distance and through the composite. In (B), a similar representation of  $R_E$  is shown when the irradiance output of LCU<sub>600</sub> was used.  $R_E$  values for less than optimal light conditions were statistically different from the optimal condition. Results obtained with the tip displacement and slight inclination are similar ( $p > 0.05$ ). The angulation of the tip caused significant changes to the energy delivered to the composite regardless of the irradiance output.

Fig. 3 shows plots for: (A) *S. mutans* counts CFU/ composite for each of irradiance output and less than optimal light conditions (mean  $\pm$  sd;  $n = 6$ ). Radiant exposure ( $R_E$ ) had a statistically significant effect ( $p = 0.0214$ ); however, less than optimal light conditions had no statistically significant influence ( $p = 0.119$ ) or interaction ( $p = 0.250$ ) via two-way ANOVA. For LCU<sub>600</sub>, Tukey's multiple comparison tests demonstrated a significant intergroup difference for moderate angulation and optimal condition with significant increased viable *S. mutans* biofilm over the cured composites by 2-fold ( $p = 0.0275$ ). The Pearson correlation between  $R_E$  and *S. mutans* biofilm formation ( $p = 0.009$ ;  $r = -0.46$ ) indicates an inverse relationship between the factors (dropping the radiant exposure led to more *S. mutans* biofilm formation).

For LCU<sub>1000</sub>, similar viability for *S. mutans* among all conditions ( $p > 0.05$ ) was observed. In (B–C), representative SEM images show bacterial adhesion and biofilm formation on the bottom surfaces of composite cylinders for LCU<sub>1000</sub> under control and moderate angulation, respectively. In (D–E) representative SEM images show increased *S. mutans* biofilm formation for LCU<sub>1000</sub> under control and moderate angulation.

The percentage DC for LCU<sub>1000</sub> at the top and bottom as a function of light conditions (mean  $\pm$  sd;  $n = 3$ ) is graphically presented in Fig. 4. In (A), the solid lines average the DC% values at the top and bottom. There was no significant difference among the DC% results on the top regardless of curing conditions. On the bottom, the moderate angulation led to the lowest DC% ( $p = 0.0158$ ). In (B), the heat maps of the average degree of conversion measured at different depths from the irradiated surface to the bottom are illustrated. The reducing %DC towards the bottom of the specimen is visualized by increasing the cold colors. A trend in reduction of the %DC was observed for groups subjected to angulations with a predominance of a green color corresponding to 50–60% of conversion.

In Fig. 5, the corresponding percentage DC at the top and bottom for LCU600 are presented. The DC% at the bottom for both angulation

groups were significantly different from the other conditions, with the main effect of irradiance ( $p < 0.001$ ) and light curing condition ( $p < 0.001$ ). The difference between the top and bottom was 34 to 52% for the groups subjected to slight and moderate angulation, respectively. Under LCU<sub>600</sub>, slight and moderate angulations have displayed the lowest DC% (34% and 10%, respectively). The impact of the reduction of DC% for these conditions can be visually observed in Fig. 5B. Cold colors (blue and purple) representing % DC values lower than 30% are noted at the bottom of the cylinder when the tip of the light curing is angulated by the operator by 35 degrees. Pearson's correlation coefficient indicated strong correlation between  $R_E$  and % DC values ( $r = 0.607$ ;  $p = 0.003$ ).

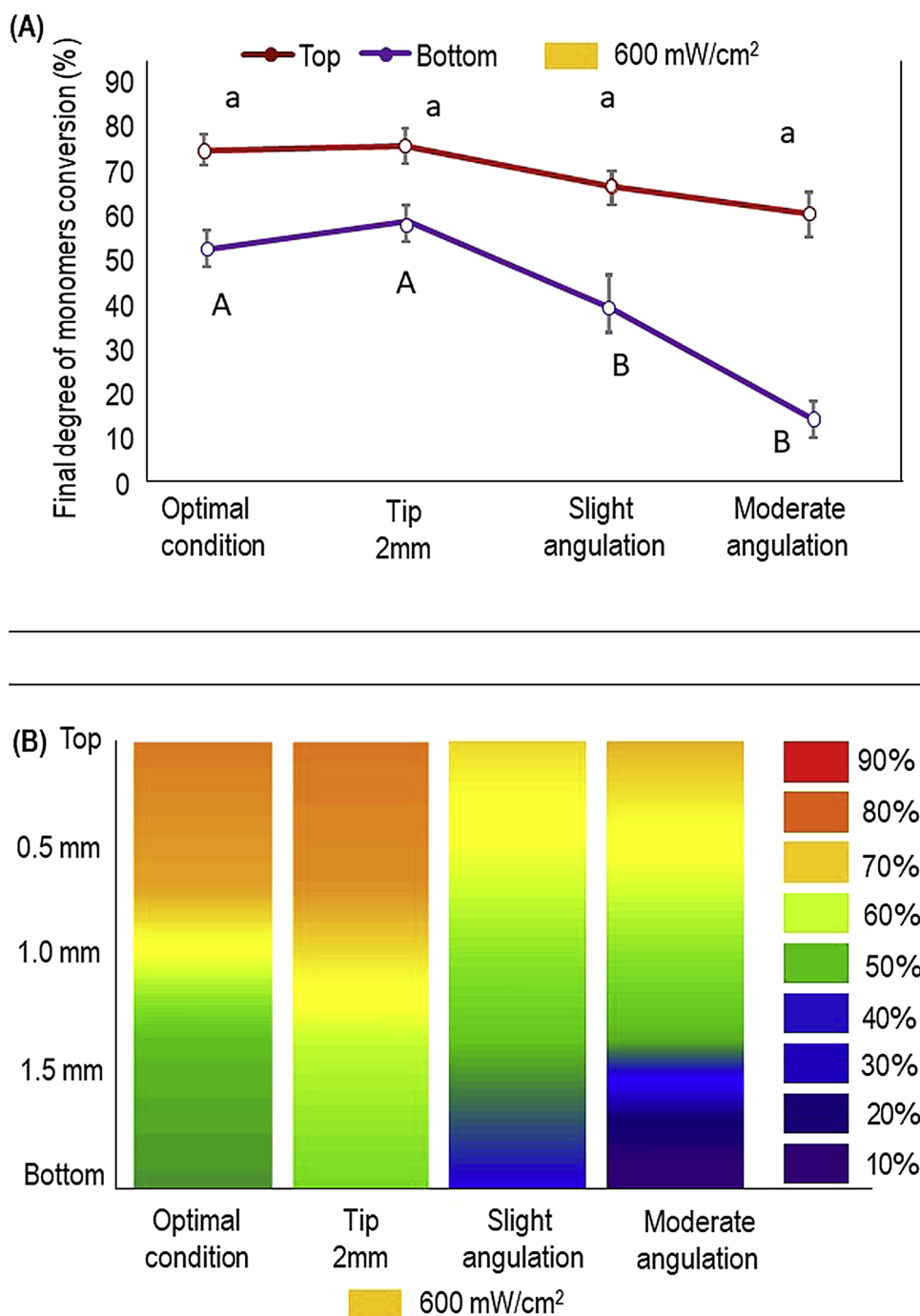
The mean and standard deviation of  $\Delta Ra$  values considering the less than optimal light conditions and two irradiance outputs (mean  $\pm$  sd;  $n = 6$ ) are presented in Fig. 6. The irradiance output ( $p = 0.0032$ ) and less than optimal light conditions ( $p = 0.0101$ ) have statistically significant effect by two-way ANOVA, although no interaction was observed ( $p = 0.271$ ). Representative SEM images of the composite surface subjected to optimal and moderate angulation, respectively for LCU<sub>1000</sub> (irradiance output of  $1000\text{ mW/cm}^2$ ) (B–C) and LCU<sub>600</sub> (D–E), are also shown in Fig. 6.  $\Delta Ra$  values varied in the range of averaged 0.029 to 0.094 for all irradiance/light curing conditions. The most prominent difference was found when using an irradiance output of LCU<sub>600</sub> with a moderate angulation. The SEM images for moderate angulation show superficial degradation effects with exposed filler on the surface of the composite, suggesting a loss of resin matrix and consequent increase in the surface roughness.

Fig. 7 shows the water sorption and solubility achieved by composite samples subjected to the factors: less than optimal light conditions and irradiance (mean  $\pm$  sd;  $n = 6$ ). The first y-axis, the bubble chart shows mean values for water sorption. The two-way ANOVA indicate that the factors or interaction were not significant ( $p > 0.05$ ). On the second y-axis, the lines show the percentage mean values for solubility. No significant differences were observed among the groups.

### 4. Discussion

Light curing procedures have gained a pole position in all dental operations as all dental adhesives, adhesive cement, and resin composites use light energy for comprehensive polymerization, which eventually contributes to the clinical success of a composite restoration. However, light curing is often taken for granted, as case complexity and technique skills take all the attention away. The polymerization of dental composites and its influencing role in the dental plaque build up is critical to understand the detrimental factors that may lead to premature failures at the margins of restorations [19]. Our data suggest that greater bacterial colonization on tested composites was primarily caused by the less than optimal curing conditions, which triggered a snowball effect driving increased water sorption and solubility, high degradation and increased roughness of composites. The different levels of irradiance/light curing unit and radiant exposure promoted by underperformed curing conditions interfered with *S. mutans* biofilm formation (CFU), the degree of conversion (DC), and the surface roughness (SR) except the water sorption and solubility, where an increasing on the trend was observed. Therefore, the hypothesis tested was partially rejected.

Clinical curing conditions are often less than optimal and vary according to the different challenges posed by the particular case. The clinical complexity explains why *in vitro* tests done under optimal conditions often do not correlate with clinical performance. During the restoration of class II preparations in posterior teeth, the placement of the light guide over the cusp tip is subjected to inclinations and displacement, among other challenges that decrease access of the light curing tip. Operator-related factors heavily impact the amount of energy received by the composite, as previously shown [22–24,28]. Our approach was to model light curing conditions in the clinical scenario



**Fig. 5.** The percentage and differences of the final DC for LCU600 at the top and bottom in function of downgrade light conditions (mean ± sd; n = 3). In (A), the solid lines average the DC% values at the top and bottom. Lower case letters compare DC at the top, while capital case letters compare DC at the bottom. Dissimilar letters are significantly different ( $p < 0.05$ ). In (B), the heat map representing the DC% measured along the composite from top to bottom. The impact of the reduction of DC% when the tip of the light curing is angulated by the operator by 35 degrees can be highlighted in this image by abundant presence of cold colors.

and provide more accurate predictions of clinical outcomes, as it relates to bacterial colonization and short-term degradation.

The loss of total energy expressed here as radiant exposure ( $R_E$ ), from LCU tip measurement at maximum simulated less than optimal light tip position is expressive. Overall, in the optimal condition, only 50–53% of the light reaches a depth of 2 mm (Fig. 2). At the simulated condition when the tip of the light curing is angulated by the operator by 35 degrees, only 27–32% of the light was recorded by the sensor. A portion of this reduction is certainly due to light scattering by the composite, and it also varies significantly among brands, but most of the attenuation can be attributed to the fact that the tip of the LCU was

pointing in the wrong direction. In the outcomes of this study: degree of conversion (%DC) at the bottom, colony-forming units (CFU) and surface roughness ( $\mu\text{m}$ ), the different inclination conditions led to even greater  $R_E$  loss than compared to the 2-mm displacement of the tip. The tip distance follows the inverse-square law where light energy varies with the inverse square of the distance between the composite and the tip of the light guide [22]. However, inclination conditions represent an even worst-case scenario. A composite surface directly facing a light source receives the maximum flux of light; but as the occlusal plane rotates, the amount of light striking a unit area, and hence the amount of light energy reflected, diminishes in proportion to the cosine of the

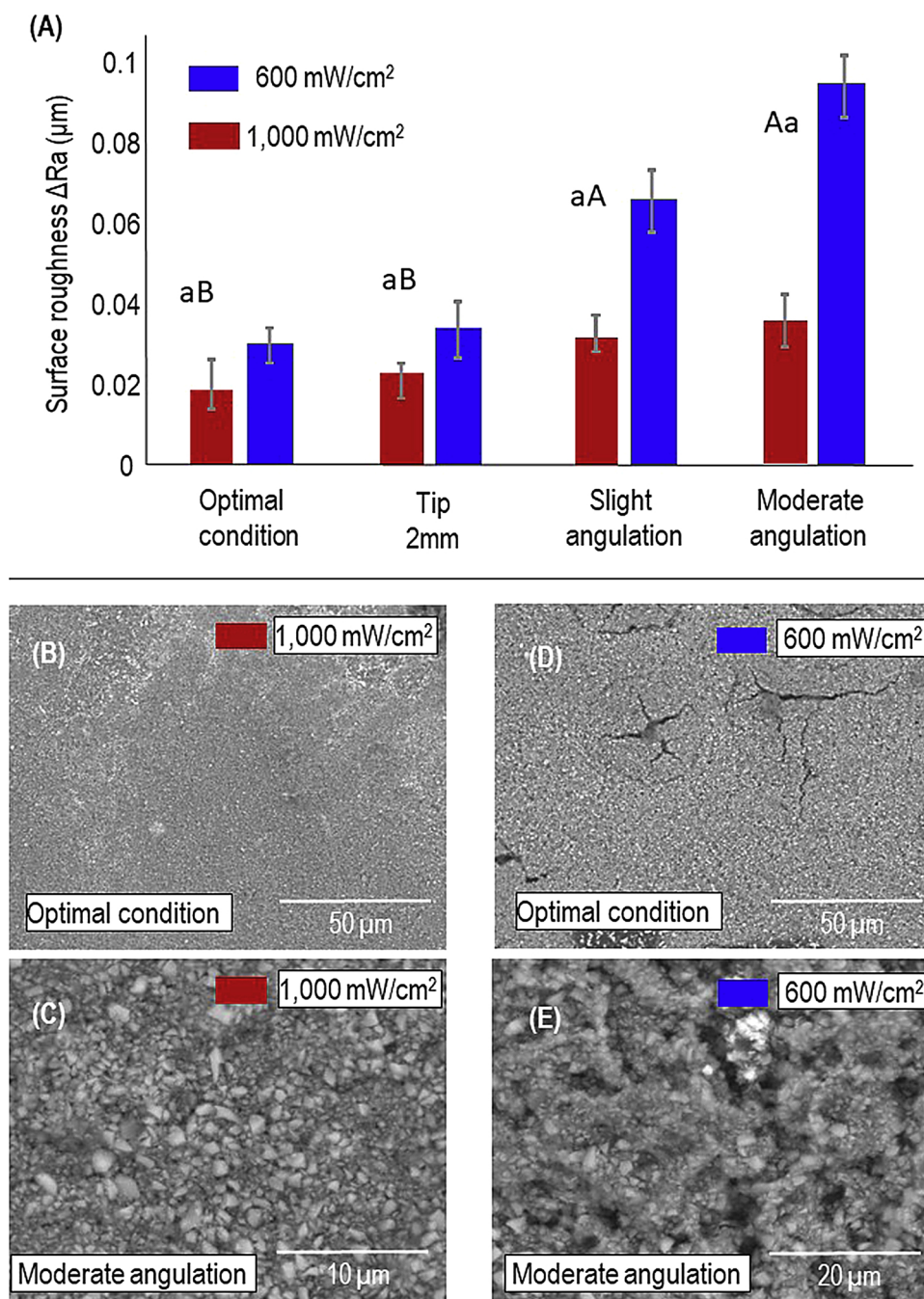


**Fig. 6.** The mean and standard deviation of  $\Delta Ra$  values considering the downgrade light conditions and two irradiance output (mean  $\pm$  sd; n = 6) are presented in Fig. 6. \* p < 0.05 compared to all other groups by two-way ANOVA; Holm-Sidak. Representative SEM images composite surface under control and moderate angulation, respectively for irradiance output of 1000 mW/cm<sup>2</sup> (B–C) and LCU600 (D–E).

angle of rotation [23,29]. In our moderate inclination condition, a plane inclined at 35 degrees to the direction of light captures approximately one-quarter the light energy that the occlusal plane directly facing the light source captures.

For biofilm growth, the results of this study suggest a moderate negative correlation with  $R_E$ . *S. mutans* species have been shown to hydrolyze resin composites and adhesives presenting specific activity toward the nitrophenyl esters [19]. The less than optimal condition by moderate angulation led to more prominent bacterial growth on the composite surface irradiated with LCU<sub>600</sub>. After 14 days of incubation, surface roughness analysis and SEM analysis showed increased surface roughness for the moderate angulation conditions compared to the control. Although quantification of released monomers was not the

focus of our study, the increased solubility results are likely due to an increased amount of residual monomers [16,17]. Previous studies also have validated surface degradation and changes in the surface topography as resulting from the *S. mutans* degradative potential [10–12].

It is unsurprising that the  $R_E$  has an impact on the degree of conversion, particularly, the conversion at the bottom of the composite since the literature has extensively covered this relationship [24,30]. However, the cascade effect of high percentage of uncured monomers on the chain of events correlated to *S. mutans* growth should be considered. The biofilm model was performed in 14 days of biofilm accumulation, a timeframe necessary for reproducing the dental caries process. Over time, biofilm thickness, change in structure, density and decreased diffusivity contribute to a diminished effect of uncured

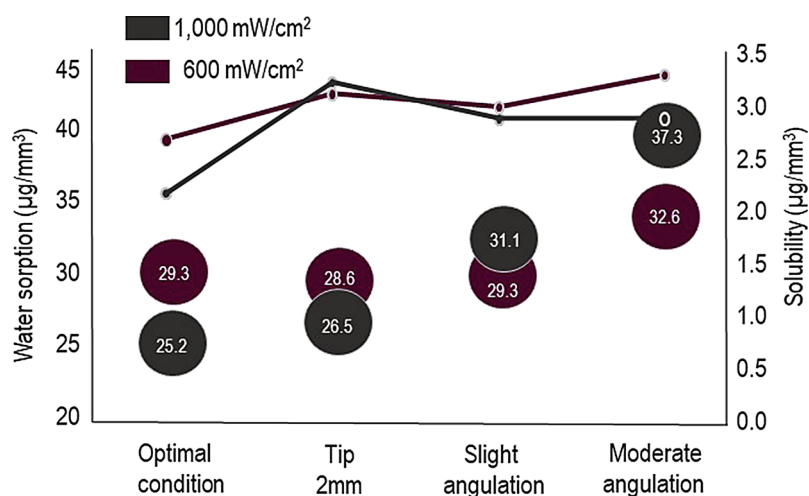


Fig. 7. Mean values for sorption and solubility reached by composite samples subjects to the factors: downgrade light conditions and irradiance (mean  $\pm$  sd; n = 6). The first y-axis, the bubble chart shows mean values for water sorption. On the second y-axis, the lines show percentage mean values for solubility. The analysis of variance has shown no significant difference for the factors and interactions although it is observed increased values for water sorption in the moderate angulation.

monomers. Also, the number of sub-products released from uncured monomers is mostly observed within seven days with no significant distinction from release after 30 days [29,31]. Therefore, the decreased conversion, and likely, increased unreacted monomer release from the materials, must have affected biofilm formation in the early stages, exactly when the virulent genes need to be expressed. In this study, the results seem to support the up-regulation of virulent genes, given the increased biofilm formation with the lower conversion of the material.

Light unit source and the curing regimen have been suggested to influence the water sorption [25]. However, after seven days of being immersed in water, the composite specimens subjected to moderate angulation showed highest water uptake and solubility for both used light source although the data were not statically significant. The observed trend in these outcomes can be related to inadequate polymerization demonstrated by the low degree of conversion for the light curing condition with greater inclination. The lack of major significance can be attributed to individual kinetic of water uptake that occurs in the organic resin matrixes. The kinetics of water sorption can be slower for some resins and may not reach equilibrium even after several days. It also can be considered the effect of filler content as the hydrolytic stability of coupling agents also varied in the different fillers.

Further investigations are needed to clarify the role of composite resin degradation products as a function of conversion and material composition on the interaction between composites and caries-related bacteria. Likewise, different light curing sources reproduce patterns [31,32] that differ from those shown by this data. Therefore, there is a compelling argument for preclinical models to consider curing parameters in identifying many important effects of relevance to bacterial metabolism and biofilm formation over composites.

In summary, the present study demonstrates increased biofilm formation as a result of sub-optimal light curing conditions. The detrimental impact imposed by the inadequate light curing on the likelihood of bacterial surface colonization is considered within the chain of events (less than optimal light curing, uncured monomers, and finally surface degradation). Under the tested conditions, the results show that the extension of detrimental effects on composites via the measured properties was strongly dependent on irradiance and light curing conditions. When light curing is contemplated, the sub-optimal light energy delivery by angulation and the irradiance of LCU<sub>600</sub> could contribute to the overall deterioration of composite and a trend in promoting the bacterial proliferation that may contribute to the progression of secondary caries.

#### 4.1. Conclusion

Less than optimal light curing using different irradiance has a

suggested role as an initial trigger of detrimental responses with increased biofilm formation on the surface of resin composites. Optimization of the curing procedures is essential to ensure maximum performance of resin-based materials and reduce the risk factors of secondary caries development.

#### Conflict of interest statement

No conflict of interest.

#### Acknowledgments

This study was supported by a seed grant from the University of Maryland School of Dentistry (MM). We gratefully acknowledge the staff of the HS/HSL Innovation Space (University of Maryland Baltimore) for their support in helping us with the design and printing templates and the Biomaterial and Tissue Engineering Division for the use of its facilities.

#### References

- [1] N. Zhang, M.A. Melo, M. Weir, M.A. Reynolds, Y. Bai, H.H. Xu, Do dental resin composites accumulate more oral biofilms and plaque than amalgam and glass ionomer materials? *Materials* 9 (2016) 888.
- [2] J. Singh, P. Khalichi, D.G. Cvitkovitch, J.P. Santerre, Composite resin degradation products from BisGMA monomer modulate the expression of genes associated with biofilm formation and other virulence factors in *Streptococcus mutans*, *J. Biomed. Mater. Res. A* 88 (2) (2009) 551–560.
- [3] L. Sadeghinejad, D.G. Cvitkovitch, W.L. Siqueira, J.P. Santerre, Y. Finer, Triethylene glycol up-regulates virulence-associated genes and proteins in *Streptococcus mutans*, *PLoS One* 11 (11) (2016) e0165760.
- [4] P. Spencer, Q. Ye, J. Park, E.M. Topp, A. Misra, O. Marangos, Y. Wang, B.S. Bohaty, V. Singh, F. Sene, J. Eslick, K. Camarda, J.L. Katz, Adhesive/dentin interface: the weak link in the composite restoration, *Ann. Biomed. Eng.* 38 (June (6)) (2010) 1989–2003.
- [5] U. Pallesen, J.W. van Dijken, A randomized controlled 27 years follow up of three resin composites in Class II restorations, *J. Dent.* 43 (December (12)) (2015) 1547–1558.
- [6] U. Pallesen, J.W. van Dijken, A randomized controlled 30 years follow up of three conventional resin composites in Class II restorations, *Dent. Mater.* 31 (October (10)) (2015) 1232–1244.
- [7] C.S. Pfeifer, Polymer-based direct filling materials, *Dent. Clin. North Am.* 61 (4) (2017) 733–750.
- [8] L.G. Lovell, S.M. Newman, C.N. Bowman, The effects of light intensity, temperature, and comonomer composition on the polymerization behavior of dimethacrylate dental resins, *J. Dent. Res.* 78 (August (8)) (1999) 1469–1476.
- [9] W.M. Palin, J.G. Leprince, M.A. Hadis, Shining a light on high volume photocurable materials, *Dent. Mater.* 34 (5) (2018) 695–710.
- [10] J.L. Drummond, Degradation, fatigue, and failure of resin dental composite materials, *J. Dent. Res.* 87 (2008) 710–719.
- [11] N. Beyth, R. Bahir, S. Matalon, A.J. Domb, E.I.S. Weiss, *Mutans* biofilm changes surface - topography of resin composites, *Dent. Mater.* 24 (6) (2008) 732–736.
- [12] Y. Takahashi, S. Imazato, R.R. Russell, Y. Noiri, S. Ebiu, Influence of resin monomers on growth of oral streptococci, *J. Dent. Res.* 83 (2004) 302–306.

- [13] N.J. Lin, C. Keeler, A.M. Kraigsley, J. Ye, S. Lin-Gibson, Effect of dental monomers and initiators on *Streptococcus mutans* oral biofilms, *Dent. Mater.* 34 (5) (2018) 776–785.
- [14] L. Sadeghinejad, D.G. Cvitkovitch, W.L. Siqueira, J. Merritt, J.P. Santerre, Y. Finer, Mechanistic, genomic and proteomic study on the effects of BisGMA-derived biodegradation product on cariogenic bacteria, *Dent. Mater.* 33 (February (2)) (2017) 175–190.
- [16] Y. Takahashi, S. Imazato, R.R. Russell, Y. Noiri, S. Ebisu, Influence of resin monomers on growth of oral streptococci, *J. Dent. Res.* 83 (2004) 302–306.
- [17] M. Hagio, M. Kawaguchi, W. Motokawa, K. Miyazaki, Degradation of methacrylate monomers in human saliva, *Dent. Mater. J.* 25 (2006) 241–246.
- [18] P. Khalichi, J. Singh, D.G. Cvitkovitch, J.P. Santerre, The influence of triethylene glycol derived from dental composite resins on the regulation of *Streptococcus mutans* gene expression, *Biomaterials* 30 (4) (2009) 452–459.
- [19] F.F. Demarco, K. Collares, M.B. Correa, M.S. Cenci, R.R. Moraes, N.J. Opdam, Should my composite last forever? Why are they failing? *Braz. Oral Res.* 31 (suppl 1) (2017) e56.
- [20] B. Huang, W.L. Siqueira, D.G. Cvitkovitch, Y. Finer, Esterase from a cariogenic bacterium hydrolyzes dental resins, *Acta Biomater.* 15 (71) (2018) 330–338.
- [21] A.P. Fugolin, L. Correr-Sobrinho, A.B. Correr, M.A. Sinhoreti, R.D. Guiraldo, S. Consani, Influence of irradiance on Knoop hardness, degree of conversion, and polymerization shrinkage of nanofilled and microhybrid composite resins, *Gen. Dent.* 64 (2) (2016) 26–31.
- [22] C. Shimokawa, B. Sullivan, M.L. Turbino, C.J. Soares, R.B. Price, Influence of emission Spectrum and irradiance on light curing of resin-based composites, *Oper. Dent.* 42 (5) (2017) 537–547.
- [23] K.L. Konerding, M. Heyder, S. Kranz, A. Guellmar, A. Voelpel, D.C. Watts, K.D. Jandt, B.W. Sigusch, Study of energy transfer by different light curing units into a class III restoration as a function of tilt angle and distance, using a MARC Patient Simulator (PS), *Dent. Mater.* 32 (5) (2016) 676–686.
- [24] C.B. André, G. Nima, M. Sebold, M. Giannini, R.B. Price, Stability of the light output, oral cavity tip accessibility in posterior region and emission Spectrum of light-curing units, *Oper. Dent.* (April) (2018) 9, <https://doi.org/10.2341/17-033-L> [Epub ahead of print].
- [25] A.L. Faria-E-Silva, C. Fanger, L. Nguyen, D. Howerton, C.S. Pfeifer, Impact of material shade and distance from light curing unit tip on the depth of polymerization of composites, *Braz. Dent. J.* 28 (5) (2017) 632–637.
- [26] T.N. Rahim, D. Mohamad, H. Md Akil, I. Ab Rahman, Water sorption characteristics of restorative dental composites immersed in acidic drinks, *Dent. Mater.* 28 (6) (2012) e63–70.
- [27] J.W. Stansbury, S.H. Dickens, Determination of double bond conversion in dental resins by near infrared spectroscopy, *Dent. Mater.* 17 (January (1)) (2001) 71–79.
- [28] R.B. Price, M.E. McLeod, Felix CM quantifying light energy delivered to a class I restoration, *J. Can. Dent. Assoc.* 76 (2) (2010) 10701.
- [29] R.B. Price, A.C. Shortall, W.M. Palin, Contemporary issues in light curing, *Oper. Dent.* 39-1 (2014) 4–14.
- [30] S.M. Cokic, R.C. Duca, J. De Munck, P. Hoet, B. Van Meerbeek, M. Smet, L. Godderis, K.L. Van Landuyt, Saturation reduces in-vitro leakage of monomers from composites, *Dent. Mater.* 34 (4) (2018) 579–586.
- [31] W. Gernscheid, L.G. de Gorre, B. Sullivan, C. O'Neill, R.B. Price, D. Labrie, Post-curing in dental resin-based composites, *Dent. Mater.* 34 (September (9)) (2018) 1367–1377.
- [32] T. Haenel, B. Hausnerová, J. Steinhaus, R.B. Price, B. Sullivan, B. Moeginger, Effect of the irradiance distribution from light curing units on the local micro-hardness of the surface of dental resins, *Dent. Mater.* 31 (February (2)) (2015) 93–104.